Title

Proteomic analyses of primary human villous trophoblasts exposed to flame retardant BDE-47 using SWATH-MS

Authors

Chen, Hao
Williams, Katherine E
Kwan, Elaine Y
et al.

Publication Date

2023-08-01

DOI

10.1016/j.tox.2023.153583

Peer reviewed

HHS Public Access

Author manuscript

Toxicology. Author manuscript; available in PMC 2024 August 01.

Published in final edited form as:

Toxicology. 2023 August 01; 494: 153583. doi:10.1016/j.tox.2023.153583.

Proteomic analyses of primary human villous trophoblasts exposed to flame retardant BDE-47 using SWATH-MS

Hao Chen[*],
Katherine E. Williams,
Elaine Y. Kwan,
Mirhan Kapidzic,
Kenisha A. Puckett,
Ali San,
Susan J. Fisher,
Joshua F. Robinson

Center for Reproductive Sciences and Department of Obstetrics, Gynecology, and Reproductive Sciences, University of California, San Francisco (UCSF), San Francisco, CA, USA

Abstract

Polybrominated diphenyl ethers (PBDEs) are a class of brominated flame retardants and recognized developmental toxicants that are detectable in placental tissues. Higher levels of in utero PBDE exposure have been associated with an increased risk of adverse birth outcomes. During pregnancy, cytotrophoblasts (CTBs) from the placenta play critical roles in the formation of the maternal-fetal interface via uterine invasion and vascular remodeling. The differentiation of these cells towards an invasive phenotype is crucial for proper placental development. We previously have shown that BDE-47 can impact CTB viability and hinder the ability of these cells to migrate and invade. To expand on potential toxicological mechanisms, we utilized quantitative proteomic approaches to identify changes in the global proteome of mid-gestation primary human CTBs after exposure to BDE-47. Using sequential window acquisition of all theoretical fragment-ion spectra (SWATH), we identified 3024 proteins in our CTB model of differentiation/invasion. Over 200 proteins were impacted as a function of BDE-47 exposure (1 μM and 5 μM) across the treatment period (15, 24, and 39 h). The differentially expressed molecules displayed time- and concentration-dependent changes in expression and were enriched in pathways associated with aggregatory and adhesive processes. Network analysis identified CYFIP1, a molecule previously unexplored in a placental context, to be dysregulated at BDE-47

[*]Correspondence to: Center for Reproductive Sciences, Department of Obstetrics, Gynecology, and Reproductive Sciences, University of California, San Francisco (UCSF), 513 Parnassus Ave, Rm. 1621, San Francisco, CA 94143-0665, USA., hachen@ionisph.com (H. Chen).

Declaration of Competing Interest

The authors declare that they have no known competing financial interests or personal relationships that could have appeared to influence the work reported in this paper.

Ethics approval

All methods were approved by the UCSF Institutional Review Board.

Appendix A. Supporting information

Supplementary data associated with this article can be found in the online version at doi:10.1016/j.tox.2023.153583.

concentrations previously seen to impact CTB migration/invasion. Our SWATH-MS dataset thus demonstrates BDE-47 impacts the global proteome of differentiating CTBs and serves as a valuable resource for further understanding of the relationship between environmental chemical exposures and placental development and function.

Availability of data and material: Raw chromatograms are deposited on the MassIVE proteomic database (https://massive.ucsd.edu) under accession number MSV000087870. Normalized relative abundances are also available as Table S1.

Keywords

Flame retardants; Cytotrophoblasts; Proteomics; Placenta

1. Introduction

Polybrominated diphenyl ethers (PBDEs) are synthetic brominated compounds that were widely used in consumer goods until their phase-out in 2004 over toxicity concerns. Although their use is restricted, levels of PBDEs persist in both environmental and human matrices (Varshavsky et al. 2020b; Zota et al. 2013). Thus, they are also found in the placenta and embryo/fetus during pregnancy (Zota et al. 2018b). Epidemiological studies report an association between *in utero* PBDE exposure and adverse developmental outcomes, particularly in neurobehavioral performance (Vuong et al. 2018). The potential impact of environmental exposures can have on pregnancy outcomes are of an additional concern (Rager et al. 2020; Stillerman et al. 2008). Pregnant women are exposed to PBDEs through various routes, including dietary sources (Schecter et al. 2006), dust (Lorber, 2008), and hand-to-mouth transfer (Buttke et al. 2013). Geographic and ethnic differences can also contribute to differential PBDE exposures (Varshavsky et al. 2020b).

During pregnancy persistent organic pollutants, including PBDEs, partition into the placenta (National Children's Study Placenta et al. 2014). The placenta, an embryonic/fetal organ, is essential for normal development due to its critical functions. For example, syncytiotrophoblasts (STBs), which form the surface of the placenta, produce a myriad of hormones and transport nutrients, gases, and wastes between the maternal and fetal circulations. Abnormal placentation is associated with adverse pregnancy outcomes and can increase the risk of chronic diseases (Burton et al. 2016). Numerous pregnancy complications with a placental origin, such as preeclampsia or placental accreta spectrum disorder, can be traced to cytotrophoblast (CTB) dysfunction (Fisher, 2015). CTBs are specialized placental cells that are critical for: 1) physically connecting the placenta and the uterus by invading the decidua and superficial myometrium; and 2) remodeling the resident arteries and rerouting maternal blood to STBs. These dynamic processes are highly spatiotemporally regulated; a CTB subpopulation differentiates and invades the uterus, where they seek out maternal spiral arteries and veins (Maltepe and Fisher, 2015). Consequently, perturbations at any stage of CTB differentiation could interfere with proper placental development.

Primary cultures of villous CTBs recapitulate the migratory and invasive processes observed in vivo (Red-Horse et al. 2004), with changes in the expression of numerous key molecules

observable on the transcriptomic level (Robinson et al. 2017b). We previously demonstrated that BDE-47 induces significant changes in the transcriptome and methylome of primary human CTBs (Robinson et al. 2019). This environmental chemical (EC) BDE-47 also significantly inhibits CTB migratory and invasive function, suggesting CTBs are sensitive to these flame retardants. A key approach in systems toxicology is the integration of different -omics datasets to better characterize and understand molecules and pathways that generate an adverse outcome (Hartung et al. 2017). Mass spectrometry-based approaches provide a highly sensitive and accurate means of making quantitative comparisons among proteomes at a global level (Titz et al. 2014). Improved instrumentation and methodologies such as SWATH-MS (Sequential Window Acquisition of All Theoretical Mass Spectra), which utilizes the strengths of label-free, data-independent acquisition, have significantly advanced proteomics (Gillet et al. 2012).

Here we report the application of SWATH-MS to assess BDE-47 effects on the global proteome of differentiating CTBs in a human cell culture model of placentation. Building on our previous transcriptomic analysis with a parallel study design (Robinson et al. 2019) and previous proteomic characterization of the model (Chen et al. 2021), we focused on defining the differential expression of proteins that could disrupt CTB migration and invasion. Our protein-level findings provide a framework for understanding the impact of BDE-47 on CTB differentiation and reinforce the biological plausibility of deleterious effects of PBDE exposures on the developing placenta.

2. Material and methods

2.1. Chemical reagents

BDE-47 (2,2′4,4′-tetrabromodiphenyl ether, >99%, CAS #5436-43-1, AccuStandard) were dissolved in dimethyl sulfoxide (DMSO, Sigma-Aldrich). Chemical treatments were introduced at a 1:1000 (vol/vol) dilution for all studies. Concentrations were selected based on our previous studies and were non-cytotoxic (Robinson et al. 2019).

2.2. Tissue collection

All methods were approved by the UCSF Institutional Review Board. Informed consent was obtained from all donors. Four second trimester placentas (gestational weeks 20–23) were collected following elective terminations and placed in cytowash medium (DME/H-21 (Gibco), 12.5% fetal bovine serum (Hyclone), 1% glutamine plus (Atlanta Biologicals), 1% penicillin/streptomycin (Invitrogen), and 0.1% gentamicin (Gibco)). Fetal sex determination was not performed. Tissue samples were stored on ice approximately an hour prior to cell isolation.

2.3. Human primary villous cytotrophoblast culture

Cytotrophoblasts (CTBs) were isolated as previously described (Robinson et al. 2017a). CTBs were cultured on precoated Matrigel (BD Biosciences) plates at a density of 104,167 cells/cm^2 in DME/H-21, 2% Nutridoma (Roche), 1% sodium pyruvate (Sigma), 1% HEPES buffer (Invitrogen), 1% GlutaminePlus (Atlanta Biologicals), and 1% penicillin/streptomycin (Invitrogen). Cells were incubated at 37 °C in 5% CO_2/95% air. Cell culture purity was

determined with cytokeratin-7 immunostaining (rat polyclonal; 1:100 (Damsky et al. 1992)). Relative trophoblast purity above 85% was required for subsequent experimentation. Time points (15, 24, and 39 hr) were selected based on previous studies evaluating the course of differentiation/invasion of CTBs (Chen et al. 2021; Robinson et al. 2017b). CTBs were exposed to 1 or 5 μM of BDE-47 1 hr after plating. Extrapolating exposure levels between in vitro and *in utero* suggests tested doses represent approximately ~3 orders of magnitude greater than geometric mean concentrations reported in placental tissues (Nanes et al., 2014; Zota et al., 2018); however, accounting for factors that influence sensitivity (e.g. lipid content of the placenta, length of exposure, life-stye factors), these tested ranges may nevertheless be relevant to human exposures (Park et al., 2020).

2.4. Protein extraction and digestion

Cultured CTBs (1×10^6 cells/condition) were washed 1X with PBS and detached with Trypsin (~5 min incubation) at 15, 24, and 39 hr, then centrifuged at 800 g for 5 min. Supernatant was removed and the cell pellet washed with 2X times with PBS, centrifuging after each wash. Cell pellets were then snap-frozen and stored at − 80°C. To extract peptides for mass spectrometry, samples were thawed then sonicated in lysis buffer (1% SDS in 50 mM ammonium bicarbonate) and concentrations were quantified using Micro BCA (Thermo Scientific). Equal amounts of protein (25 μg) were reduced in 5 mM TCEP (tris carboxyethylphospine) at 60 °C for 45 min. Iodoacetic acid was added to the samples at a final concentration of 10 mM and for 15 min incubated at room temperature, covered. Samples were digested with trypsin (Promega) at a 1:20 ratio (w/w) and overnight at 37° C. Peptides were cleaned using the Pierce Detergent Removal Columns (Thermo Scientific) according to manufacturer's protocol.

2.5. Peptide fractionation and SWATH-MS

For library generation, peptides were fractionated using alkaline pH reversed-phase HPLC, with each of the 8 fractions injected into a nanoLC Ultra 2D Plus system (SCIEX) with the cHiPLC system interfaced to a 5600 Triple TOF mass spectrometer (SCIEX). Peptides were initially loaded onto a guard column (300 μm i.d.×5 mm,5-μm particle size, 100-Å pore size; Acclaim PepMap300 C18; Thermo-Fisher) and washed with aqueous phase solution composed of 2% solvent B [98% acetonitrile (ACN)/0.1% formic acid (FA)] prepared with solvent A (2% ACN/0.1% FA) at a flow rate of 12 μL/min for 3 min. Then, peptides were separated with a C18 Acclaim PepMap100 column (75 μm i.d.×150 mm, 3-mmparticle size, 100-Å pore size; Thermo Fisher Scientific) at 40 °C. Peptides were eluted at 300 nL/min with a gradient of 2–35% solvent B for 90 min. In positive ion mode, MS scans from 400 to 1200 *m/z* were acquired followed by MS/MS scans of the 20 most abundant ions with an exclusion time of 15 s. The spectral library was constructed by processing the raw data-dependent fractionation files through ProteinPilot™ against a human reference proteome (UniProt). SWATH-MS acquisition was performed with the instrumentation detailed above using a 50-variable-window setup. SWATH MS1 survey scans were acquired from 400 to 1200 *m/z* for 250 ms and MS2 spectra were acquired from 100 to 1500 *m/z* for 65 ms in high-sensitivity mode. We extracted information containing at least 3 transitions per peptide and 3 peptides per protein. Peak group detections were filtered at 1% FDR using the SWATH Replicates Analysis Template. Analyses were performed in SCIEX Cloud

OneOmics™ after uploading to Illumina's BaseSpace Cloud. Raw chromatogram files, including of the spectral library, can be found on the MassIVE proteomic database (https://massive.ucsd.edu) under accession number MSV000087870. Normalized abundance values were log2 transformed for downstream analysis and are available in Table S1.

2.6. Immunofluorescent staining

Tissues were fixed in 4% paraformaldehyde and dehydrated through sequential increases in sucrose before OCT embedment (Thermo Fisher Scientific). Sections were permeabilized with methanol and rinsed with PBS before incubation in blocking buffer (5% BSA, 0.05% Tween 20). CTBs were labeled with rat anti-cytokeratin 7 (1:100) (Damsky et al., 1992) and rabbit anti-CYFIP-1 (1:500) (Cell Signaling) for 1 h at 37 °C. After additional PBS washes (3X), primary antibodies were detected using species-specific secondary antibodies (1:1000, Jackson ImmunoResearch Labs, Inc). Sections were mounted using Vectashield with DAPI (Vector Laboratories). Images were acquired using a Leica DM5000 B inverted microscope. Tissue sections from 3 2nd-trimester placentas were evaluated.

2.7. Bioinformatic analysis

Gene ontology analysis was performed with EnrichR and DAVID (Dennis et al. 2003; Kuleshov et al. 2016). limma (Ritchie et al. 2015) and signaling pathway impact analysis (SPIA) (Tarca et al. 2009) were performed in R. Venn diagrams were plotted with InteractiVenn (Heberle et al. 2015). Network analysis was performed with Cytoscape (Shannon et al. 2003).

2.8. Statistics

Mass spectrometry acquisitions were analyzed and normalized using SCIEX Cloud OneOmics™. Differential expression analysis was conducted with integrated linear modeling via limma (Ritchie et al. 2015) in R; proteins with a false discovery adjusted p-value of $p < 0.05$ were considered significant. Gene ontology analysis was conducted with a modified Fisher's Exact test through DAVID or Enrichr using the study's dataset as a reference background. Heatmaps were generated with MeV (MultiExperiment Viewer) (Howe et al. 2010). Graphs were created in R and Graphpad.

3. Results

3.1. Dataset characteristics

A simplified diagram of our SWATH-MS workflow is diagrammed in Fig. 1A. 3024 unique proteins were identified in our SWATH-MS datasets across all timepoints. The relative protein abundances spanned five orders of magnitude (Fig. 1B) with comparable levels of variation among the four vehicle-treated biological replicates (Fig. 1C).

3.2. Differential expression analysis of proteins impacted by BDE-47 exposure

In total, 203 proteins were differentially expressed (DE) ($p < 0.05$) as a result of BDE-47 treatment in a concentration- and time-dependent manner (Fig. 2A), with the majority being upregulated. Enrichment analysis of the DE proteins identified overrepresentation

of annotated processes related to “neutrophil degranulation” and “homotypic cell-cell adhesion,” “cadherin binding,” and “focal adhesion” ($p < 0.01$) (Fig. 2B). DE proteins included those associated with putative mechanisms of BDE-47 toxicity, such as the upregulation of markers of inflammation/oxidative stress (*NFKB1, PRDX2/3*), and those modulated during CTB differentiation such as the integrin cell-extracellular matrix receptors (*ITGA1, ITGB1, ILK*).

To distinguish the most impacted biomolecules at each condition (“robust expression” changes), cutoffs were imposed (log fold change≥|1|, $p < 0.05$) (Fig. 3A). Full expression profiles of these 59 robustly changing proteins were also plotted as a heatmap (Fig. 3B). The number of unique proteins with robust expression changes from BDE-47 treatment (59 unique proteins) increased with culture time (Fig. S1A). In general, there was limited overlap between these proteins at each condition (Fig. S1B). Three proteins showed elevated expression at all time points as a function of increased BDE-47 concentration at 5 μM (*SH3BGRL2, SNX17, MAP1LC3*) (Fig. S2A,B) and another three proteins showed expression above the cutoff starting after 15 hr (*BUD31, MAN2B2, TOR1A*) (Fig. S2C,B), suggesting a temporal influence of exposure on select biomolecules impacted by BDE-47.

3.3. Temporal and concentration-dependent effects of BDE-47 on CTB protein expression

Clustered dot plots of the robustly changing DE proteins at each time point revealed a bias toward upregulation (Fig. 4A–C). At 15 hr, few robustly changed proteins were shared between 1 μM and 5 μM treatments, suggesting a concentration-dependent effect on protein expression during the initial culture period. By 24 hr more overlapping proteins with robust changes observed at both 1 μM and 5 μM suggested a trend toward shared response pathways. Interestingly, at 24 hr there was also a greater number of highly significant DE proteins at 1 μM vs. 5 μM (13 additional proteins). At 39 hr there remained an overlap of proteins affected at both BDE-47 concentrations but an increase in those unique to 1 μM or 5 μM emerged. Additionally, more DE proteins at 39 hr had larger expression changes compared to earlier culture periods, highlighting the impact of longer periods of chemical treatments in vitro.

3.4. Network analyses of BDE-47 affected CTB proteins

Our previous studies demonstrated that BDE-47 significantly inhibits cytotrophoblast migration and invasion (Robinson et al. 2019). To explore the potential molecules involved, network analysis (Cytoscape) of DE proteins was performed and specific subsections were highlighted based on significant functional enrichments ($p < 0.01$). As multiple studies suggest oxidative stress contribute to PBDE toxicity (Costa and Giordano, 2007), we focused our efforts on the NF-κB node and its associated molecules at 5 μM, a concentration of BDE-47 that inhibited CTB migration and invasion in our prior studies. CYFIP1, which our study identified as one of the most significant and robustly changing molecules, was among the neighboring nodes of interest (Fig. 5A). Immunostaining of second trimester placental biopsies revealed CYFIP1 staining at the maternal-fetal interface, including invading CTBs at the implantation site, suggesting an unexplored role in placentation and the potential of BDE-47 to impact its regulation (Fig. 5B).

4. Discussion

While legislative efforts have broadly phased out PBDEs in consumer products, their persistence in human tissues (Cowell et al. 2018), including the placenta (Varshavsky et al. 2020a), represents a matter of toxicological interest. Our findings support the hypothesis that PBDEs can interfere with protein expression in human CTBs and that numerous pathways, including those associated with CTB migration and invasion, may be impacted by these exposures. These results extend previous observations from our group and others that the placenta is vulnerable to PBDE exposures.

Associations between increased inflammatory markers and PBDE exposures in pregnant women have previously been observed (Zota et al. 2018a). Similarly, placental cell lines exposed to BDE-47 exhibit increased reactive oxygen species (ROS) production and proinflammatory cytokine release, suggesting the placenta is both a contributor to, and target of, inflammation (Park et al. 2014). It was theorized that NF-κB may be involved in BDE-47 induced cytokine release, since its activation is linked to responses in ROS and stimulation of proinflammatory receptors (Morgan and Liu (2011)). Our mass spectrometry data lends additional credence to this hypothesis, as NF-κB was one of the most statistically significant DE proteins following BDE-47 treatment. Our findings also extend previous observations that BDE-47 suppresses CTB migration and invasion, in our group and others (Park et al. 2020), by the identification of proteins which could be involved in these processes, such as CYFIP1, a subunit of the WAVE complex that promotes epithelial cell adhesion and suppresses tumorigenesis (Silva et al. 2009). TNFα-driven NF-κB activation —and downstream MMP-9 expression—require the WASF3 complex, which interacts with CYFIP1 (Teng et al. 2011; Teng et al. 2016). This protein's role in CTB development has not been previously explored and further experiments utilizing genetic manipulation are necessary. However, two observations suggest the possibility that important CTB functions such as aggregation and invasion are likely inhibited early, and CYFIP1 may play a role during this period. Robust CYFIP1 upregulation occurs early on in culture as measured by mass spectrometry, during the timeframe when CTB migration and aggregation is the most active (Robinson et al. 2017b). While expression changes in proteins were most robust at 39 hr, including those of numerous cytoskeletal-associated proteins were upregulated in our dataset at 39 hr (e.g. *MAP1LC3B, MAP1S, ITGA1*), it represents a period when aggregation and invasion is completed and BDE-47-treated CTBs do not show significant differences in CYFIP1 expression compared to vehicle control. These observations are supported by signaling pathway analysis of the 203 significantly DE proteins, which revealed perturbations ($p < 0.05$) only of the "sulfur relay system" at 15 hr. Although a number of proteins that regulate the actin cytoskeleton were DE, there was a notable but nonsignificant inhibition at the pathway level at 15 hr ($p = 0.071$) at 5 μM but no significant changes at later time points (Table S2). Whether these observations in the placenta is similar across different gestational ages remains to be elucidated.

The breadth of data from toxicoproteomics studies yields numerous mechanistic avenues that were not fully explored in this work; interestingly, of the 203 proteins that were significantly impacted by BDE-47 exposure only 32 had overlap with those that drive basal CTB differentiation determined from our previous study (Chen et al. 2021). Other

regulators of motility and invasiveness from the DE list, such as *SLFN5* or *SCIN*, may contribute to BDE-47 driven CTB inhibition. Furthermore, the impact of BDE-47 on the exosomal pathway is of intrigue. An appreciable number of the DE proteins from BDE-47 treatment contained an “extracellular exosome” annotation via DAVID (82/203 ≈40.3%). As the proteome of exosomes from placental tissues can be significantly altered with environmental chemical exposure (Sheller-Miller et al. 2020) and exosomal release from CTBs can affect the surrounding decidual environment (Taylor et al. 2020), these interactions may deleteriously influence proper development during pregnancy.

Previous investigations examining select morphological biomarkers of PBDE exposure in mid-gestation placenta samples yielded inconclusive results (Varshavsky et al. 2020a). The findings of this study highlight the complexity of the CTB differentiation process and the potential challenges in linking biomolecule expression to subtle exposure outcomes. The placenta remains an understudied organ with unknowns, especially in the context of environmental health and toxicology. Continued research of placental development will improve risk characterization, as a clearer understanding of the underlying biomolecules that regulate its biology will increase confidence in candidate identification. Additionally, further exploration regarding fetal sex as a risk factor is warranted. Complementary -omics approaches, such as transcriptomics and proteomics, combined with human relevant models such as the primary villous CTB system, represent promising exploratory measures in that regard. This study’s findings provide a framework, at the global proteome level, of BDE-47′s effects on CTBs and reinforces the potential hazard it and similar classes of compounds may pose on the placenta.

Supplementary Material

Refer to Web version on PubMed Central for supplementary material.

Funding

This work was kindly supported by the National Institutes of Environmental Health Sciences (NIEHS) K99ES030401 [H.C], R00ES023846 [J.F.R], and P30ES030284-01A1 [Tracey Woodruff., S.J. F.]).

Data availability

Data uploaded and provided in public repository.

References

Burton GJ, Fowden AL, Thornburg KL, 2016. Placental origins of chronic disease. Physiol. Rev. 96 (4), 1509–1565. [PubMed: 27604528]

Buttke DE, Wolkin A, Stapleton HM, Miranda ML, 2013. Associations between serum levels of polybrominated diphenyl ether (pbde) flame retardants and environmental and behavioral factors in pregnant women. J. Expo. Sci. Environ. Epidemiol. 23 (2), 176–182. [PubMed: 22760441]

Chen H, Williams KE, Kwan EY, Kapidzic M, Puckett KA, Aburajab RK, Robinson JF, Fisher SJ, 2021. Global proteomic analyses of human cytotrophoblast differentiation/invasion. Dev. (Camb., Engl.) 148 (13).

Costa LG, Giordano G, 2007. Developmental neurotoxicity of polybrominated diphenyl ether (pbde) flame retardants. Neurotoxicology 28 (6), 1047–1067. [PubMed: 17904639]

Cowell WJ, Sjödin A, Jones R, Wang Y, Wang S, Herbstman JB, 2018. Determinants of prenatal exposure to polybrominated diphenyl ethers (pbdes) among urban, minority infants born between 1998 and 2006. Environ. Pollut. 233, 774–781 (Barking, Essex: 1987). [PubMed: 29127935]

Damsky CH, Fitzgerald ML, Fisher SJ, 1992. Distribution patterns of extracellular matrix components and adhesion receptors are intricately modulated during first trimester cytotrophoblast differentiation along the invasive pathway, in vivo. J. Clin. Investig. 89 (1), 210–222. [PubMed: 1370295]

Dennis G Jr., Sherman BT, Hosack DA, Yang J, Gao W, Lane HC, Lempicki RA, 2003. David: Database for annotation, visualization, and integrated discovery. Genome Biol. 4 (5), P3. [PubMed: 12734009]

Fisher SJ, 2015. Why is placentation abnormal in preeclampsia? Am. J. Obstet. Gynecol. 213 (4 Suppl), S115–S122. [PubMed: 26428489]

Gillet LC, Navarro P, Tate S, Rost H, Selevsek N, Reiter L, Bonner R, Aebersold R, 2012. Targeted data extraction of the ms/ms spectra generated by data-independent acquisition: A new concept for consistent and accurate proteome analysis. Mol. Cell. Proteom.: Mcp. 11 (6). O111 016717.

Hartung T, FitzGerald RE, Jennings P, Mirams GR, Peitsch MC, Rostami-Hodjegan A, Shah I, Wilks MF, Sturla SJ, 2017. Systems toxicology: Real world applications and opportunities. Chem. Res. Toxicol. 30 (4), 870–882. [PubMed: 28362102]

Heberle H, Meirelles GV, da Silva FR, Telles GP, Minghim R, 2015. Interactivenn: A web-based tool for the analysis of sets through venn diagrams. BMC Bioinforma. 16 (1), 169.

Howe E, Holton K, Nair S, Schlauch D, Sinha R, Quackenbush J, 2010. Mev: Multiexperiment viewer. In: Ochs MF, Casagrande JT, Davuluri RV (Eds.), Biomedical Informatics for Cancer Research. Springer US, Boston, MA, pp. 267–277.

Kuleshov MV, Jones MR, Rouillard AD, Fernandez NF, Duan Q, Wang Z, Koplev S, Jenkins SL, Jagodnik KM, Lachmann A, et al. , 2016. Enrichr: A comprehensive gene set enrichment analysis web server 2016 update. Nucleic Acids Res. 44 (W1), W90–W97. [PubMed: 27141961]

Lorber M, 2008. Exposure of americans to polybrominated diphenyl ethers. J. Expo. Sci. Environ. Epidemiol. 18 (1), 2–19. [PubMed: 17426733]

Maltepe E, Fisher SJ, 2015. Placenta: The forgotten organ. Annu. Rev. Cell Dev. Biol. 31, 523–552. [PubMed: 26443191]

Morgan MJ, Liu Z.-g, 2011. Crosstalk of reactive oxygen species and nf-κb signaling. Cell Res 21 (1), 103–115. [PubMed: 21187859]

National Children's Study Placenta C, Nanes JA, Xia Y, Dassanayake RMAPS, Jones RM, Li A, Stodgell CJ, Walker C, Szabo S, Leuthner S, et al. , 2014. Selected persistent organic pollutants in human placental tissue from the united states. Chemosphere 106, 20–27. [PubMed: 24485817]

Park HR, Elkin ER, Castillo-Castrejon M, Loch-Caruso R, 2020. Brominated diphenyl ether-47 differentially regulates cellular migration and invasion in a human first trimester trophoblast cell line. Reprod. Toxicol. 93, 191–198. [PubMed: 32142752]

Park HR, Kamau PW, Loch-Caruso R, 2014. Involvement of reactive oxygen species in brominated diphenyl ether-47-induced inflammatory cytokine release from human extravillous trophoblasts in vitro. Toxicol. Appl. Pharmacol. 274 (2), 283–292. [PubMed: 24296301]

Rager JE, Bangma J, Carberry C, Chao A, Grossman J, Lu K, Manuck TA, Sobus JR, Szilagyi J, Fry RC, 2020. Review of the environmental prenatal exposome and its relationship to maternal and fetal health. Reprod. Toxicol.

Red-Horse K, Zhou Y, Genbacev O, Prakobphol A, Foulk R, McMaster M, Fisher SJ, 2004. Trophoblast differentiation during embryo implantation and formation of the maternal-fetal interface. J. Clin. Investig. 114 (6), 744–754. [PubMed: 15372095]

Ritchie ME, Phipson B, Wu D, Hu Y, Law CW, Shi W, Smyth GK, 2015. Limma powers differential expression analyses for rna-sequencing and microarray studies. Nucleic Acids Res. 43 (7), e47. [PubMed: 25605792]

Robinson JF, Kapidzic M, Gormley M, Ona K, Dent T, Seifikar H, Hamilton EG, Fisher SJ, 2017a. Research resource: Transcriptional dynamics of cultured human villous cytotrophoblasts. Endocrinology.

Robinson JF, Kapidzic M, Gormley M, Ona K, Dent T, Seifikar H, Hamilton EG, Fisher SJ, 2017b. Transcriptional dynamics of cultured human villous cytotrophoblasts. Endocrinology 158 (6), 1581–1594. [PubMed: 28323933]

Robinson JF, Kapidzic M, Hamilton EG, Chen H, Puckett KW, Zhou Y, Ona K, Parry E, Wang Y, Park JS, et al. , 2019. Genomic profiling of bde-47 effects on human placental cytotrophoblasts. Toxicol. Sci.: Off. J. Soc. Toxicol. 167 (1), 211–226.

Schecter A, Papke O, Harris TR, Tung KC, Musumba A, Olson J, Birnbaum L, 2006. Polybrominated diphenyl ether (pbde) levels in an expanded market basket survey of u.S. Food and estimated pbde dietary intake by age and sex. Environ. Health Perspect. 114 (10), 1515–1520. [PubMed: 17035135]

Shannon P, Markiel A, Ozier O, Baliga NS, Wang JT, Ramage D, Amin N, Schwikowski B, Ideker T, 2003. Cytoscape: A software environment for integrated models of biomolecular interaction networks. Genome Res. 13 (11), 2498–2504. [PubMed: 14597658]

Sheller-Miller S, Radnaa E, Arita Y, Getahun D, Jones RJ, Peltier MR, Menon R, 2020. Environmental pollutant induced cellular injury is reflected in exosomes from placental explants. Placenta 89, 42–49. [PubMed: 31675489]

Silva JM, Ezhkova E, Silva J, Heart S, Castillo M, Campos Y, Castro V, Bonilla F, Cordon-Cardo C, Muthuswamy SK, et al. , 2009. Cyfip1 is a putative invasion suppressor in epithelial cancers. Cell 137 (6), 1047–1061. [PubMed: 19524508]

Stillerman KP, Mattison DR, Giudice LC, Woodruff TJ, 2008. Environmental exposures and adverse pregnancy outcomes: A review of the science. Reprod. Sci. (Thousand Oaks, Calif.) 15 (7), 631–650.

Tarca AL, Draghici S, Khatri P, Hassan SS, Mittal P, Kim JS, Kim CJ, Kusanovic JP, Romero R, 2009. A novel signaling pathway impact analysis. Bioinformatics 25 (1), 75–82. [PubMed: 18990722]

Taylor SK, Houshdaran S, Robinson JF, Gormley MJ, Kwan EY, Kapidzic M, Schilling B, Giudice LC, Fisher SJ, 2020. Cytotrophoblast extracellular vesicles enhance decidual cell secretion of immune modulators via tnfα. Dev. (Camb., Engl.) 147 (17).

Teng Y, Liu M, Cowell JK, 2011. Functional interrelationship between the wasf3 and kiss1 metastasis-associated genes in breast cancer cells. Int J. Cancer 129 (12), 2825–2835. [PubMed: 21544801]

Teng Y, Qin H, Bahassan A, Bendzunas NG, Kennedy EJ, Cowell JK, 2016. The wasf3-nckap1-cyfip1 complex is essential for breast cancer metastasis. Cancer Res. 76 (17), 5133–5142. [PubMed: 27432794]

Titz B, Elamin A, Martin F, Schneider T, Dijon S, Ivanov NV, Hoeng J, Peitsch MC, 2014. Proteomics for systems toxicology. Comput. Struct. Biotechnol. J. 11 (18), 73–90. [PubMed: 25379146]

Varshavsky JR, Robinson JF, Zhou Y, Puckett KA, Kwan E, Buarpung S, Aburajab R, Gaw SL, Sen S, Smith SC, et al. , 2020a. Association of polybrominated diphenyl ether (pbde) levels with biomarkers of placental development and disease during mid-gestation. Environ. Health.: a Glob. Access Sci. Source 19 (1), 61.

Varshavsky JR, Sen S, Robinson JF, Smith SC, Frankenfield J, Wang Y, Yeh G, Park JS, Fisher SJ, Woodruff TJ, 2020b. Racial/ethnic and geographic differences in polybrominated diphenyl ether (pbde) levels across maternal, placental, and fetal tissues during mid-gestation. Sci. Rep. 10 (1), 12247. [PubMed: 32699379]

Vuong AM, Yolton K, Dietrich KN, Braun JM, Lanphear BP, Chen A, 2018. Exposure to polybrominated diphenyl ethers (pbdes) and child behavior: Current findings and future directions. Horm. Behav. 101, 94–104. [PubMed: 29137973]

Zota AR, Geller RJ, Romano LE, Coleman-Phox K, Adler NE, Parry E, Wang M, Park JS, Elmi AF, Laraia BA, et al. , 2018a. Association between persistent endocrine-disrupting chemicals (pbdes, oh-pbdes, pcbs, and pfass) and biomarkers of inflammation and cellular aging during pregnancy and postpartum. Environ. Int. 115, 9–20. [PubMed: 29533840]

Zota AR, Linderholm L, Park JS, Petreas M, Guo T, Privalsky ML, Zoeller RT, Woodruff TJ, 2013. Temporal comparison of pbdes, oh-pbdes, pcbs, and oh-pcbs in the serum of second trimester pregnant women recruited from san francisco general hospital, california. Environ. Sci. Technol. 47 (20), 11776–11784. [PubMed: 24066858]

Zota AR, Mitro SD, Robinson JF, Hamilton EG, Park JS, Parry E, Zoeller RT, Woodruff TJ, 2018b. Polybrominated diphenyl ethers (pbdes) and hydroxylated pbde metabolites (oh-pbdes) in maternal and fetal tissues, and associations with fetal cytochrome p450 gene expression. Environ. Int. 112, 269–278. [PubMed: 29316516]

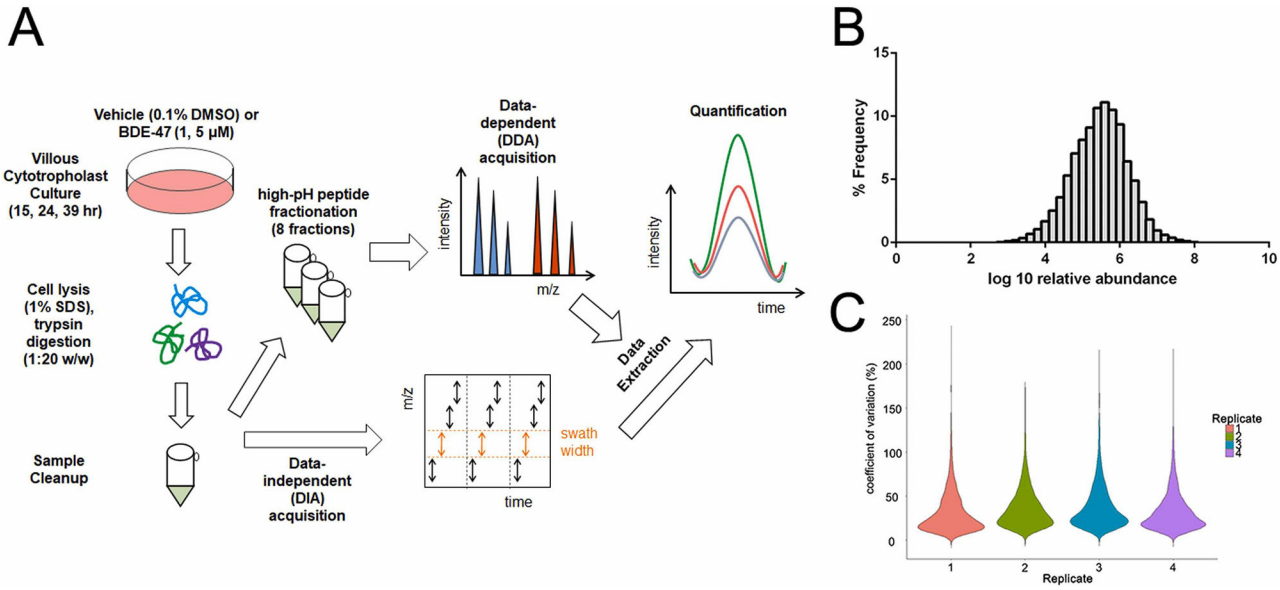

Fig. 1.

SWATH-MS dataset characteristics. A) Simplified diagram of experimental workflow. B) Frequency distribution of relative protein abundance. C) Violin plot depicting coefficient of variation between vehicle treatments of each biological replicate.

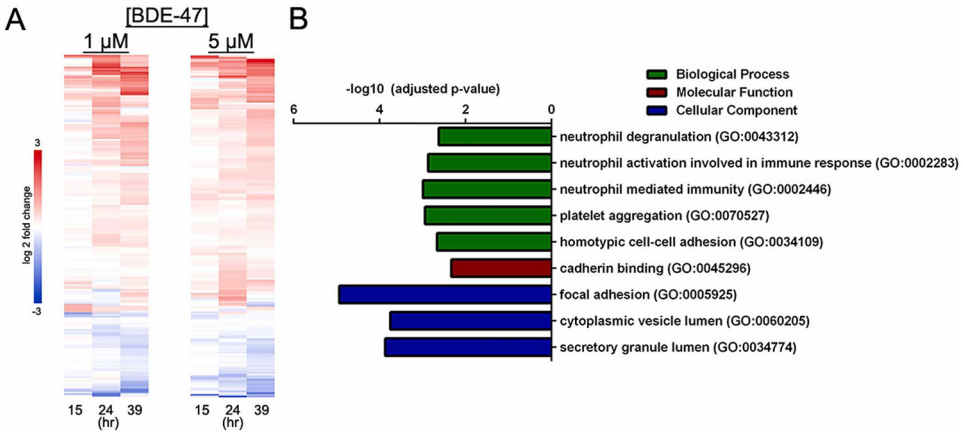

Fig. 2.

Differential expression analysis of BDE-47 treated cytotrophoblasts (CTBs). A) Clustered heatmap of relative average expression changes in CTBs exposed to BDE-47 at 1 and 5 μM after 15, 24, and 39 hr of treatment ($p < 0.05$). B) Functional annotation of enriched pathways associated with BDE-47 DE proteins using Enrichr ($p < 0.05$). n = 4.

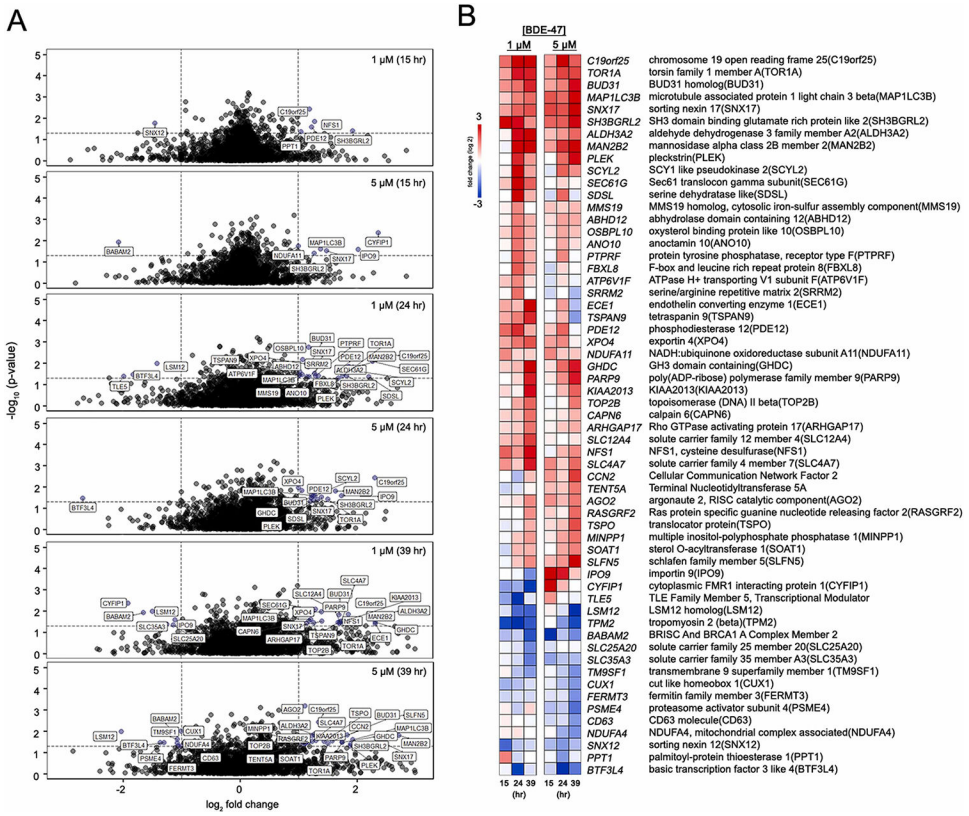

Fig. 3.

Cytotrophoblast (CTB) proteins exhibiting robust expression changes after BDE-47 treatment. A) Volcano plots depicting distribution of differentially expressed proteins at each time point (15, 24, 39 hr) and BDE-47 concentration (1 and 5 μM), highlighting proteins with robust expression changes (log fold change≥|1|, $p < 0.05$). B) Heatmap depicting the expression profiles in relative average expression of selected CTB proteins with robust changes in abundance after BDE-47 treatment. n = 4.

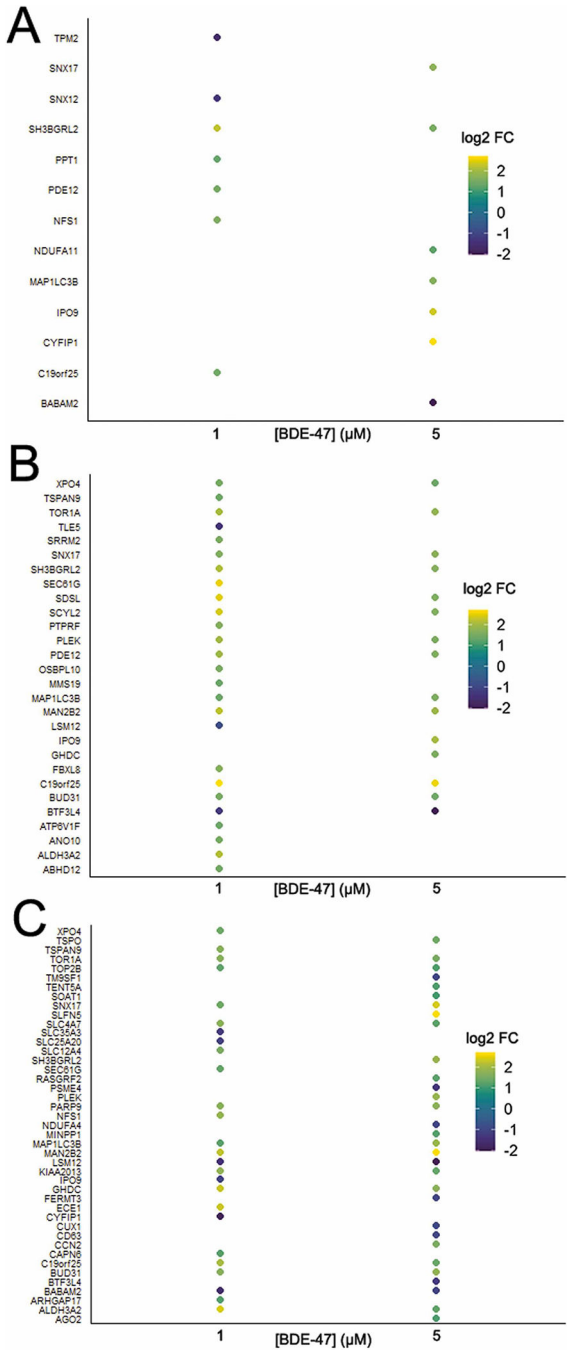

Fig. 4.

Cytotrophoblast (CTB) proteins with robust expression changes display a time- and concentration-dependence. Clustered dot plots depicting relative average expression and significance changes of BDE-47 DE proteins at A) 15, B) 24, and C) 39 hr with a log fold change≥ |1| cutoff. n = 4.

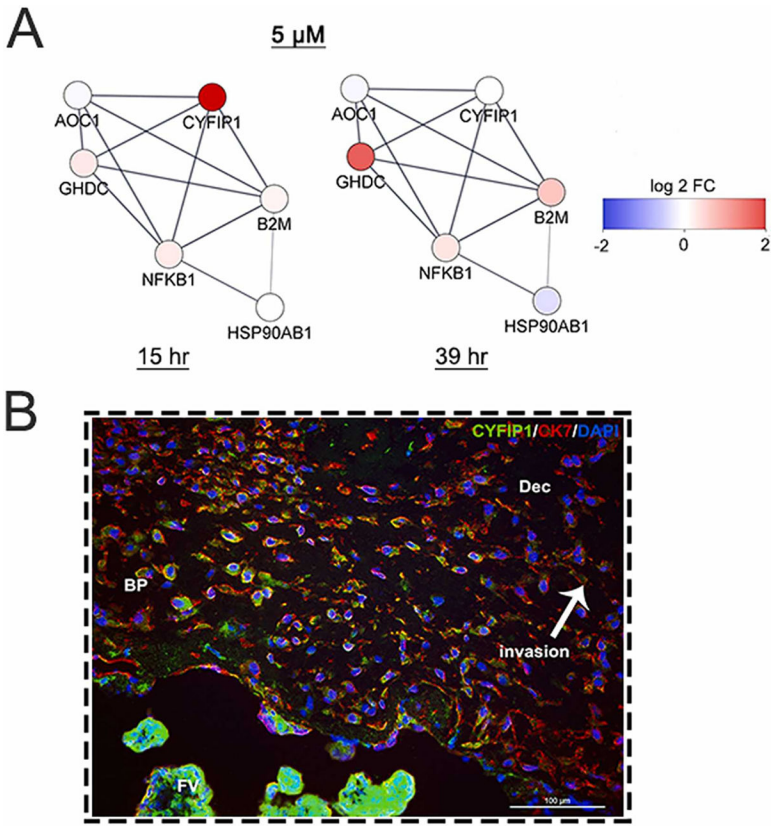

Fig. 5.

Cytoplasmic FMR1 Interacting Protein 1 (CYFIP1) expression is impacted by BDE-47. A) Visualization of predicted protein-protein network interaction with NF-κB using the STRING database with 5 μM BDE-47 treatment, at 15 and 39 hr. B) Representative image from second trimester tissue sections of the basal plate. Sections were stained with the anti-cytotrophoblast marker cytokeratin 7 (red), DAPI (blue) and CYFIP1 (green). n = 3 biological replicates. Scale bar= 100 μm. BP, basal plate; FV, floating villi; Dec, decidua.